Talanta 146 (2016) 318–325

Contents lists available at ScienceDirect

Talanta

journal homepage: www.elsevier.com/locate/talanta

Immobilization-free electrochemical DNA detection with anthraquinone-labeled pyrrolidinyl peptide nucleic acid probe

Jutatip Kongpeth [a], Sakda Jampasa [b], Piyasak Chaumpluk [c], Orawon Chailapakul [d], Tirayut Vilaivan [a,*]

[a] Organic Synthesis Research Unit, Department of Chemistry, Faculty of Science, Chulalongkorn University, Phayathai Road, Patumwan, Bangkok 10330, Thailand
[b] Program in Petrochemistry, Faculty of Science, Chulalongkorn University, Phayathai Road, Patumwan, Bangkok 10330, Thailand
[c] Laboratory of Plant Transgenic Technology and Biosensor, Department of Botany, Faculty of Science, Chulalongkorn University, Phayathai Road, Patumwan, Bangkok 10330, Thailand
[d] Electrochemistry and Optical Spectroscopy Research Unit, Department of Chemistry, Faculty of Science, Chulalongkorn University, Phayathai Road, Patumwan, Bangkok 10330, Thailand

ARTICLE INFO

Article history:
Received 15 June 2015
Received in revised form
25 August 2015
Accepted 26 August 2015
Available online 28 August 2015

Keywords:
Redox active label
Peptide nucleic acid
Electrochemical detection
DNA biosensor
Screen-printed carbon electrode

ABSTRACT

Electrochemical detection provides a simple, rapid, sensitive and inexpensive method for DNA detection. In traditional electrochemical DNA biosensors, the probe is immobilized onto the electrode. Hybridization with the DNA target causes a change in electrochemical signal, either from the intrinsic signal of the probe/target or through a label or a redox indicator. The major drawback of this approach is the requirement for probe immobilization in a controlled fashion. In this research, we take the advantage of different electrostatic properties between PNA and DNA to develop an immobilization-free approach for highly sequence-specific electrochemical DNA sensing on a screen-printed carbon electrode (SPCE) using a square-wave voltammetric (SWV) technique. Anthraquinone-labeled pyrrolidinyl peptide nucleic acid (AQ-PNA) was employed as a probe together with an SPCE that was modified with a positively-charged polymer (poly quaternized-(dimethylamino-ethyl)methacrylate, PQDMAEMA). The electrostatic attraction between the negatively-charged PNA–DNA duplex and the positively-charged modified SPCE attributes to the higher signal of PNA–DNA duplex than that of the electrostatically neutral PNA probe, resulting in a signal change. The calibration curve of this proposed method exhibited a linear range between 0.35 and 50 nM of DNA target with a limit of detection of 0.13 nM ($3SD_{blank}$/Slope). The sub-nanomolar detection limit together with a small sample volume required (20 μL) allowed detection of <10 fmol (<1 ng) of DNA. With the high specificity of the pyrrolidinyl PNA probe used, excellent discrimination between complementary and various single-mismatched DNA targets was obtained. An application of this new platform for a sensitive and specific detection of isothermally-amplified shrimp's white spot syndrome virus (WSSV) DNA was successfully demonstrated.

1. Introduction

The ability to precisely and sensitively identify specific DNA sequence has found widespread applications in many areas e.g. medical diagnostics, agricultural and food sciences [1], and environmental monitoring [2]. In addition to the direct sequencing that require expensive instrument and gel-based approaches that are labor intensive and time-consuming, various DNA sensing platforms that are more suitable for point-of-care diagnostics have been developed over the past decades [3–5]. Among these, electrochemical DNA biosensors offer several advantages including the operational simplicity, high sensitivity, miniaturization and low cost of instrument [6,7]. In general, a probe that can specifically recognize the nucleic acid target is first immobilized onto the electrode. Binding to the target results in a measurable signal change either directly or through a redox-active indicator or labels [8–14]. The most frequently employed immobilization methods include gold–thiol interaction [15–17] and amide bond formation [18,19]. The immobilization step is time-consuming, requires large excess of the probe, and needs careful optimization. Attempts were made to avoid this by using biotin-streptavidin [20,21], host–guest interaction [22], or by electrostatic adsorption [23]. Alternatively, an intercalating redox indicator [24] or a redox-active probe [25–27] had been used in combination with PCR or other

* Corresponding author. Fax: +66 22187598.
E-mail address: vtirayut@chula.ac.th (T. Vilaivan).

http://dx.doi.org/10.1016/j.talanta.2015.08.059
0039-9140/

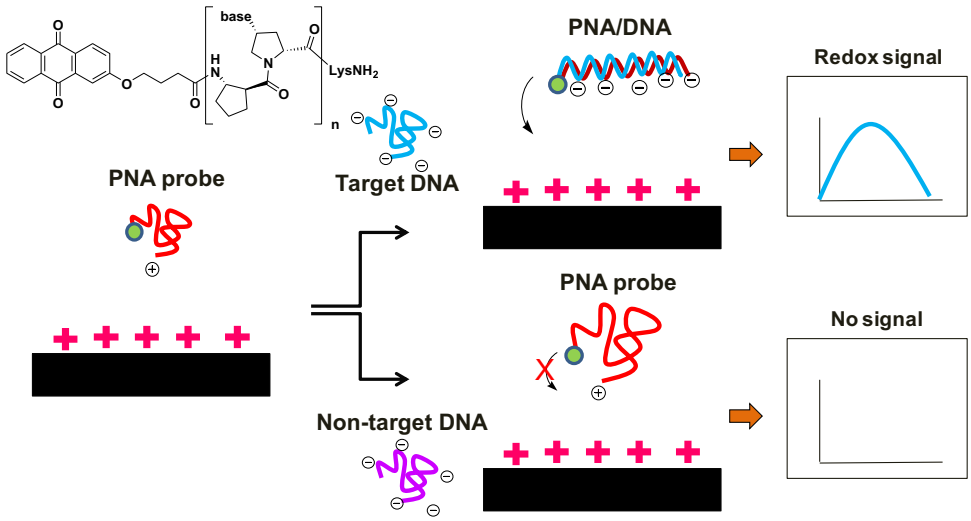

Fig. 1. The principle of immobilization-free electrochemical DNA biosensor employing AQ-PNA probe (structure of AQ-PNA shown in the inset).

enzymatic reactions for immobilization-free DNA detection.

Although DNA had been the most frequently employed probe, several new DNA analogs such as locked nucleic acid (LNA), morpholino and peptide nucleic acid (PNA) are becoming more popular alternatives because they can offer additional advantages including higher sensitivity, specificity and stability [28]. We recently reported a new conformationally constrained pyrrolidinyl peptide nucleic acid that showed excellent DNA hybridization properties [29–31] and demonstrated its applications as a probe for DNA sensing [32,33], including electrochemical detection [34–36].

The electrostatically neutral backbone of PNA allows designing of novel immobilization/detection concepts [37,38]. Luo et al. had recently developed an immobilization-free DNA sensing platform employing ferrocene-labeled PNA probes and indium-tin oxide (ITO) electrodes [39–41]. They observed that the signal detection can be switched from on-off to off-on mode by modifying the surface charge of the electrode [39]. Here we propose an immobilization-free electrochemical DNA sensing platform employing PNA and a polymer-modified screen-printed carbon electrode (SPCE), which can be easily and inexpensively prepared in one step. The electrostatic properties of the electrode can be readily controlled by adding the polymer modifier into the carbon ink without the need to form a monolayer or coating as usually the cases with other electrodes. A practical application was demonstrated in a highly specific detection of WSSV-a shrimp viral pathogen that causes large economic losses to shrimp aquaculture [42].

2. Material and methods

2.1. General materials and methods

Graphite powder (mesh size < 100) was purchased from Sigma-Aldrich. Carbon ink and silver/silver chloride were purchased from Acheson (California, USA). Other reagents and solvents were obtained from commercial suppliers and used without further purification. Poly quaternized-(dimethylamino)ethyl methacrylate (PQDMAEMA, $M_n = 1.38 \times 10^4$ Da) was synthesized and supplied by Dr. Voravee Hoven and Miss Pornpen Sae-ung (Chulalongkorn University). NMR spectra were recorded on a Bruker Avance 400 instrument operating at 400 MHz for ^{1}H and 100 MHz for ^{13}C. Chemical shifts were referenced to the residual protonated solvent peaks. MALDI-TOF MS spectra were measured on a Microflex MALDI-TOF mass spectrometer (Bruker Daltonik GmbH, Bremen, Germany) in linear positive mode using α-cyano-4-hydroxycinnamic acid (CCA) matrix. Synthetic oligodeoxynucleotides were purchased from Pacific Science (Bangkok, Thailand) and were used as received. The sequences of PNA and DNA oligonucleotides used in this study, which correspond to a partial sequence of WSSV, are as follows:

AQ-labeled WSSV PNA probe (AQ-PNA): 2AQ-CTAAATTCAGA-LysNH$_2$

Target DNA (Dcomp): 5′-TCTGAATTTAG-3′

Single base mismatched DNA (DsmC): 5′-TCTGACTTTAG-3′

Long single stranded complementary DNA (ssDcomp19):
5′-CTAAGTCTGAATTTAGGGG-3′

Long single stranded mismatched DNA (ssDsmC19):
5′-CTAAGTCTGACTTTAGGGG-3′

Long double stranded complementary DNA (dsDcomp19):
5′-CTAAGTCTGAATTTAGGGG-3′
3′-GATTCAGACTTAAATCCCC-5′

Long double stranded mismatched DNA (dsDsmC19):
5′-CTAAGTCTGACTTTAGGGG-3′
3′-GATTCAGACTGAAATCCCC-5′

Other oligonucleotides used in the specificity test include (mismatch positions underlined):

DsmC6: 5′-TCTGACTTTAG-3′ DsmA4: 5′-TCTAAATTTAG-3′
DsmG6: 5′-TCTGAGTTTAG-3′ DsmT4: 5′-TCTTAATTTAG-3′
DsmT6: 5′-TCTGATTTTAG-3′ DsmA7: 5′-TCTGAAATTAG-3′
DsmC5: 5′-TCTGCATTTAG-3′ DsmC7: 5′-TCTGAACTTAG-3′
DsmG5: 5′-TCTGGATTTAG-3′ DsmG7: 5′-TCTGAAGTTAG-3′
DsmT5: 5′-TCTGTATTTAG-3′ DsmA11: 5′-TCTGAATTTAA-3′

2.2. General procedure for synthesis and labeling of the PNA probe

The WSSV PNA probe (AQ-PNA) used in this study is a pyrrolidinyl PNA with prolyl-2-aminocyclopentanecarboxylic acid backbone (acpcPNA) with a sequence of 2AQ-CTAAATTCAGA-LysNH$_2$ (Fig. 1). The unlabeled PNA probe was synthesized by Fmoc solid-phase peptide synthesis on a TentaGel resin with a Rink amide linker following a previously described protocol [30]. The Fmoc group at the *N*-terminus of the PNA on the solid support was next removed by treatment with 2% 1,8-diazabicycloundec-7-ene (DBU) and 20% piperidine in dimethylformamide (DMF) (100 μL) for 5 min. The free PNA (0.5 μmol) was next reacted with 4-(anthraquinone-2-oxy)butyric acid (pre-activated as a pentafluorophenyl ester, 7.5 μmol) and diisopropylethylamine (DIEA) (20 μL) in DMF (100 μL). After completion of the reaction

(monitored by MALDI-TOF MS), the AQ-PNA was heated with 1:1 (v/v) aqueous ammonia:dioxane in a sealed tube at 60 °C overnight to remove the nucleobase protecting groups. Following a cleavage from the solid support with trifluoroacetic acid (TFA), the crude AQ-PNA was purified by reverse phase HPLC (C18 column, 0.1% v/v TFA in H_2O–MeOH gradient).

2.3. Preparation of the PQDMAEMA-modified screen-printed carbon electrode (PQDMAEMA-SPCE)

The SPCE used in this study consisted of a three-electrode system prepared as described previously [36,43] (Fig. S1, SI). The only difference is that the carbon ink mixture was prepared by mixing PQDMAEMA solution (1% w/v), graphite powder and carbon ink together at a ratio of 0.35:0.2:1 (0.26% w/v PQDMAEMA in the ink mixture) followed by the binder solution (1 mL/g carbon ink) and sonicated to give a homogenous mixture.

2.4. DNA extraction and amplification by Loop-Mediated Isothermal Amplification (LAMP)

DNA of total genomic and associated WSSV viral DNA was extracted via a commercialized Genomic DNA Extraction Mini Kit (RBC, USA) using 50 mg broodstock specimen. The extracted DNA specimen was amplified by LAMP [44] with a set of primers consisting of WSSV F3, WSSV B3, WSSV FIP, and WSSV BIP (Table S1). The reaction mixture consisted of 40 mM Tris pH 8.8, 20 mM KCl, 16 mM $MgSO_4$, 0.2% Tween 20, 1.6 M betaine, 2.8 mM dNTP, and 8 U *Bst* DNA polymerase. After the incubation at 63 °C for 30 min, the LAMP products were examined by electrophoresis on 3% agarose gel and visualized under a UV transilluminator after staining with ethidium bromide.

For the specificity test, four strains of shrimp virus including WSSV, Infectious Hypodermal and Hematopoietic Necrosis Virus (IHHNV), Yellow Head Virus (YHV), and Taura Syndrome Virus (TSV) were included in the specificity test (Fig. S2, SI). The WSSV and IHHNV DNA samples were extracted and amplified by LAMP as described above. For RNA viruses (YHV and TSV), total RNA was extracted based on the Nucleospin RNA kit (RBC, USA) as recommend in the manufacturer's protocol. The YHV and TSV RNA were amplified by RT-LAMP [44]. The first two viral-infected specimens were kindly provided by Chachoengsao Coastal Fisheries Research and Development Center, Chachoengsao, Thailand, and the latter two specimens were from a private hatchery in Phang Nga, Thailand.

The sensitivity of the assay was determined using equivalent copy numbers of control plasmid nucleic acid at 10-fold dilutions [45]. These samples having copy number covering from 10^7 to 10 copies were then amplified by LAMP at 63 °C for 30 min. The sensitivity of assay was analyzed and compared with standard PCR [46] via gel electrophoresis (Fig. S3, SI). To construct plasmid DNA for standard control, the DNA products corresponding to the transmembrane signal peptide gene were cloned into the TA vector as described by manufacturer (Invitrogen, Madison USA). This vector was transformed to *Escherichia coli* [47] and the nucleotide sequence was confirmed via direct nucleotide sequencing prior to use as control DNA. These plasmid DNAs were also used as a standard template of known copy number DNA.

2.5. Sample preparation and electrochemical measurement

2.5.1. Sample preparation

The concentrated stock solutions of AQ-PNA and DNA were mixed to give the desired concentration in an appropriate buffer. Twenty microliters of the AQ-PNA or AQ-PNA+DNA sample was dropped onto the PQDMAEMA-modified electrode. For double-stranded synthetic DNA and appropriately diluted LAMP samples, the AQ-PNA+DNA mixture was heated at 90 °C for 10 min and was cooled to room temperature before the measurement.

2.5.2. Electrochemical measurement

Electrochemical measurements were carried out on the PQDMAEMA-modified SPCE (surface area of the working electrode = 0.16 cm^2) by using PGSTAT 30 potentiostat (Metrohm Siam Company Ltd., Switzerland) and controlled with the General Purpose Electrochemical System (GPES) software version 4.9 (Eco Chemie B.V., Utrecht, The Netherlands). Unless otherwise specified, all measurements were conducted using a square-wave voltammetric method at room temperature (25 °C) in 10 mM Tris–HCl buffer pH 8.0. The redox signal was measured by SWV, with baseline subtraction. The measured signals are shown as average of three independent measurements ± standard deviations.

2.5.3. Optimization of parameters

For optimization of SWV parameters (amplitude, step potential and frequency), the SPCE prepared from 0.26% PQDMAEMA-modified carbon ink was used. The initial concentration of the AQ-PNA probe and DNA targets was 50 μM and was decreased to 50 nM during the optimization steps.

2.5.4. Specificity test and effects of excess non-target DNA

Specificity test was performed by measurement of the SWV signals of various mismatched DNA (see the sequence in Section 2.1) (50 nM) after hybridized with the AQ-PNA probe (50 nM) in 10 mM Tris–HCl buffer (pH 8.0) under the optimized conditions. Effects of excess non-target DNA to the signal of PNA and complementary PNA–DNA hybrid were studied with AQ-PNA (50 nM) and complementary DNA (Dcomp) (50 nM or 0 nM), in the presence of non-target DNA (DsmC) (0, 50, 500 and 5000 nM) in 10 mM Tris–HCl buffer (pH 8.0) under the optimized conditions.

2.5.5. Reproducibility test

Six PQDMAEMA-modified electrodes were prepared with the same process, and the signal was measured in the presence of AQ-PNA and complementary DNA (50 nM each) under the optimized conditions. Percent relative standard deviations (%RSD) were calculated according to Eq. (1), where SD is the standard deviation of current signal.

$$\%RSD = (SD/mean) \times 100 \quad (1)$$

3. Results and discussion

3.1. Synthesis and characterization of the AQ-PNA probe

Anthraquinone [48,49] was chosen as the redox active reporter group in this study because of its simple structure and excellent chemical stability. The carboxy-containing anthraquinone label 4-(anthraquinone-2-oxy)butyric acid was synthesized from commercially available 2-hydroxyanthraquinone (see details in Supporting information) and was characterized spectroscopically (Fig. S4-S6). It was next coupled to the PNA at the N-terminus to install the anthraquinone label. The *m/z* value of unlabeled PNA probe was 3844.2 (calcd *m/z* = 3842.2) and that of the AQ-PNA was 4134.5 (calcd *m/z* = 4134.3) (Fig. S7, SI). The mass increase of 290 Da corresponds to the AQ label, thus it can be concluded that the redox-active reporter AQ was successfully incorporated into the PNA probe. The purity of the AQ-PNA was confirmed to be > 90% by reverse phase HPLC (Fig. S8, SI)

Melting temperature (T_m) of the hybrid between the AQ-

Table 1
Thermal stability data of AQ-PNA: 2AQ-CTAAATTCAGA-LysNH$_2$ after hybridized with various DNA.

DNA	Sequence (5′→3′)	T_m (°C)[a]	ΔT_m[b]
Dcomp	TCTGAATTTGA	82.7	22.2
DsmC	TCTGAC<u>T</u>TTGA	60.5	
Dcomp19	CTAAGTCTGAATTTAGGGG	> 90 (83.7)[c]	> 20 (22.7)[c]
DsmC19	CTAAGTCTGAC<u>T</u>TTAGGGG	70.5 (61.0)[c]	

[a] T_m was measured in 10 mM sodium phosphate buffer pH 7.0, [PNA]=[DNA]= 1.0 μM.
[b] T_m (complementary hybrid) – T_m (single base mismatched hybrid).
[c] Values in parenthesis were obtained in the presence of 100 mM NaCl.

labeled probe and its complementary DNA was 82.7 °C, which was higher than the corresponding DNA hybrid with the unlabeled probe (80.0 °C). Furthermore, the T_m value of the AQ-PNA decreased by more than 20 °C when hybridized with single base mismatched DNA (60.5 °C). These results (Table 1) indicate that the AQ-PNA probe binds to DNA with high affinity and specificity.

3.2. Preliminary electrochemical characterization of AQ-PNA probe

To test the possibility of using the labeled PNA as a probe for immobilization-free electrochemical detection of DNA sequence, the single stranded AQ-PNA was subjected to a SWV measurement on an unmodified SPCE that was pre-conditioned in 0.5 M aqueous NaOH at 1.3 V for 30 s [50]. A redox peak was observed at –0.71 V which corresponds well to that of the free AQ label (Fig. S9, SI). After hybridization with the complementary DNA target (Dcomp), the signal was completely suppressed. Hybridization with the single base mismatched DNA (DsmC) resulted in less signal suppression. It was hypothesized that the unmodified electrode possesses a negatively-charged surface after conditioning due to partial oxidation of the electrode surface to form carboxylate groups [50]. This can electrostatically interact with the AQ-PNA (carrying a positively-charged lysine residue) but not the corresponding PNA–DNA hybrid (negatively-charged due to the phosphate groups), resulting in the observed signal change.

3.3. Preparation and characterization of PQDMAEMA-modified electrode

It was proposed that if the electrode was first modified to provide a positively-charged surface, an electrochemical detection should be possible according to the principle shown in Fig. 1.

According to Fig. 1, no signal of the labeled PNA probe should be observed due to the unfavorable electrostatic interaction between the free AQ-PNA probe and the positively-charged electrode. Upon binding to the complementary DNA, the negatively-charged PNA–DNA hybrid should electrostatically attract to the electrode surface, allowing efficient electron transfer, resulting in a detectable electrochemical signal. A related concept for signal on PNA-based electrochemical DNA detection had been previously performed on a poly(allylamine hydrochloride) (PAH)-coated indium tin oxide (ITO) electrode [39].

In this work, a much simpler approach was proposed whereby the positively-charged polymer was mixed into the carbon ink mixture to be used for screening of the electrode [51]. Chitosan was previously incorporated into the SPCE to provide a handle for immobilization of the PNA probe [36]. Since chitosan contains positively-charged amino groups, we proposed that chitosan could be employed to provide positive charges on the electrode. Although a preliminary experiment confirmed that the immobilization-free electrochemical DNA detection was possible with the chitosan-modified SPCE, the limited solubility and operating pH range of chitosan [52] prompted us to find a more suitable candidate. The positively-charged quaternized polymer PQDMAEMA was found to be the most suitable polymer and was selected as the modifier in all subsequent studies. In a control experiment (Fig. S10, SI), the SWV signal at –0.78 V corresponding to the anthraquinone label in AQ-PNA was observed only when the complementary DNA was present and not in bare electrode, AQ-PNA or DNA alone, thus validating the concept proposed in Fig. 1.

3.4. Optimization of parameters and calibration curve

First, the buffer was optimized by comparing the SWV signals between free and hybridized probes (with complementary and mismatched DNA) and Tris–HCl buffer pH 8.0 was chosen (Fig. S11, SI). To determine the optimal amount of the polymer modifier, the percentage of the polymer in the carbon ink mixture to be used for the electrode screening was varied from 0.13% to 5.2% w/v and the electrochemical signal of the PNA probe was measured in the absence and presence of the complementary DNA target (Fig. S12, SI). Increasing the polymer amount resulted in higher signals, but also higher backgrounds. The carbon ink containing 0.26% PQDMAEMA was chosen for the next studies because it gave the best compromise between the signal and background. The performances of unmodified and PQDMAEMA-modified SPCE were also evaluated by cyclic voltammetry. At identical scan rate, the signal of $[Fe(CN)_6]^{3-/4-}$ was stronger in the PQDMAEMA-modified electrode, which is to be expected based on its positively-charged nature. The signal of $[Fe(CN)_6]^{3-/4-}$ increased as a linear function of square root of scan rate, providing linearity in the range of 0.2–0.6 V s^{-1} with R^2=0.9974 and 0.9986 for oxidation and reduction processes, respectively (Fig. S13, SI). The results imply that the oxidation and reduction of the redox active reporter on these modified electrodes is diffusion controlled. However, when the target DNA or PNA–DNA duplex are present, they may strongly adsorb onto the electrode surface, which makes the conclusion based on the response to $[Fe(CN)_6]^{3-/4-}$ not applicable.

By employing 50 nM AQ-PNA–DNA hybrids on 0.26% PQDMAEMA-modified SPCE, the optimal SWV parameters including frequency 40 Hz, step potential 0.0075 V and amplitude 100 mV were identified (Fig. S14, SI). At 50 nM AQ-PNA probe concentration, the measured SWV signal showed a logarithmic relationship with the concentration of complementary DNA (Dcomp) (Fig. 2A). The calibration curve exhibited a linear range between 0.35 and 50 nM of DNA (log scale) with R^2=0.9757 (Fig. 2B). At high concentrations of DNA, the signal decreased (at 350 nM, the signal was approximately 50% of the maximum signal at 50 nM) which can be explained by a competitive adsorption of the excess unhybridized DNA (vide infra, Section 3.6). The limit of detection (LOD), as calculated from 3 times the ratio between the standard deviation of the blank signal and slope of the calibration graph was 0.13 nM (130 pM). The single mismatched DNA target (DsmC) yielded signals that are indistinguishable from the background at all concentrations tested. The sub-nanomolar LOD are comparable to other non-amplified electrochemical DNA detection platforms that employ covalently-labeled redox-active probes [11,53], see also Table 2. The small sample volume required (20 μL) means that the total amount of detectable DNA sample is small (LOD < 10 fmol or < 1 ng for 300nt ssDNA). This is considerably better than the detection limit obtained from the PAH-modified ITO electrode by Luo et al. (40 fmol) [39]. Although not the best by electrochemical detection standard, this level of sensitivity is better than what can be achieved by optical dyes commonly used in gel staining (1–50 ng of DNA), and is more than sufficient for detection of real DNA samples obtained from PCR or other suitable amplification methods. Moreover, the quantity of the probe required for each measurement (50 nM, 20 μL or 1 pmol) was also

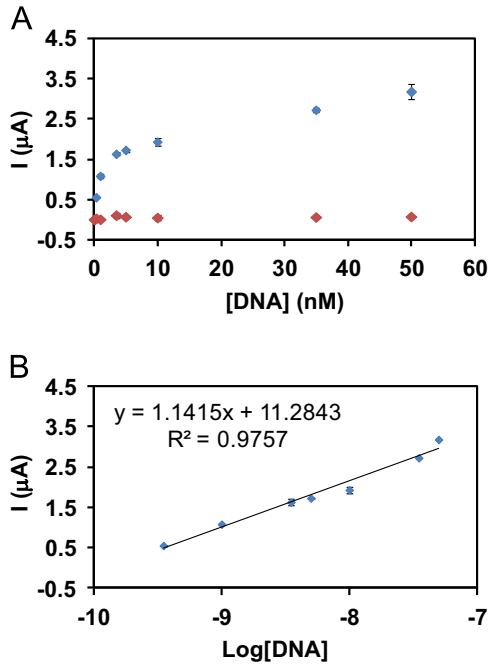

Fig. 2. (A) Scan of linear range of AQ-PNA (50 nM) after addition of complementary DNA (blue) and non-complementary DNA (red) at 0.1, 0.35, 1, 3.5, 5, 10, 35 and 50 nM (total volume=20 μL in 10 mM Tris–HCl buffer pH 8.0) on PQDMAEMA-modified SPCE (polymer content 0.26% in the carbon ink composition before screening) under optimized conditions (frequency 40 Hz, step potential 0.075 V, amplitude 0.100 V) (B) same as (A), but the concentrations were expressed in log scale. (For interpretation of the references to color in this figure legend, the reader is referred to the web version of this article.)

much smaller than the typical concentration required for probe immobilization (μM range), and the hybridization and the measurement take only a few minutes to complete.

It should be noted that the sensor exhibits satisfactory reproducibility. Since the screen-printed carbon electrodes employed are disposable type, only the electrode-to-electrode reproducibility was calculated at 50 nM AQ-PNA probe and two concentrations of DNA at low and high ends of the linearity range (3.5 nM and 35 nM). The percent relative standard deviations (RSD) of 9.06% and 8.50% were obtained at 3.5 and 35 nM DNA, respectively.

3.5. Specificity of AQ-PNA probe

Specificity is one of the most important aspects in DNA sequence detection. The specificity of this new immobilization-free PNA-based platform was investigated with several DNA targets containing a single base mismatch in the sequence at various positions. From Fig. 3, it is clear that the developed DNA sensing platform exhibits excellent specificity without the requirement for elevated temperature [39], addition of organic co-solvents [56], or more elaborated design [57]. The signal was observed only with complementary DNA and the mismatched DNA DsmA11 carrying a single base mismatched at the 3′-end of the strand. This is not unexpected considering the small difference in stabilities of complementary and terminal mismatched hybrids [58]. All other single base mismatched DNA targets gave virtually no detectable signal, hence it is important to design the probe that include the hotspot towards the middle of the sequence for single mismatch discrimination purposes. The high specificity of the sensor can be attributed to the high specificity of the pyrrolidinyl PNA probe (acpcPNA) used. The large difference in stability (ΔT_m=22 °C, see Table 1) means that the mismatched PNA–DNA hybrid is much less stable than the complementary hybrid, and therefore cannot

Table 2
Comparison of performance of the present work with previous works.

Electrode[a]	Probe[b]	Detection	Linear range	Detection limit	References
ITO	19nt Fc-labeled PNA (non-immobilized)	DPV	0.25×10^{-6}–2×10^{-6} M	0.25×10^{-6} M	[39]
PAH/ITO	19nt Fc-labeled PNA (non-immobilized)	DPV	20×10^{-9}–100×10^{-9} M	20×10^{-9} M	[39]
ITO	11nt Fc-labeled PNA and 47nt hairpin-forming oligonucleotide (non-immobilized)	DPV (with DNA polymerase-assisted target recycling)	0.1×10^{-9}–20×10^{-9} M	0.1×10^{-9} M	[27]
ITO	28nt MB-labeled hairpin DNA oligonucleotide (non-immobilized)	DPV (with Exonuclease III-assisted target recycling)	20×10^{-12}–0.3×10^{-9} M	20×10^{-12} M	[26]
ITO	37nt Fc-labeled hairpin DNA oligonucleotide (non-immobilized)	DPV (with Exonuclease III-assisted autocatalytic target recycling)	0.1×10^{-12}–0.1×10^{-9} M	0.1×10^{-12} M	[54]
AuE	77nt Fc-labeled hairpin DNA oligonucleotide with streptavidin aptamer region (non-immobilized)	SWV (with polymerase/nicking-induced isothermal signal amplification)	5×10^{-15}–10×10^{-12} M	2.56×10^{-15} M	[55]
Poly(p-phenylenediamine)-AuE	9–12nt unlabeled acpcPNA (immobilized)	Capacitive	1×10^{-12}–1×10^{-8} M	0.2×10^{-12} M	[34]
Chitosan-modified SPCE	14nt AQ-labeled acpcPNA (immobilized)	SWV	0.02×10^{-6}–12×10^{-6} M	4×10^{-9} M	[36]
PQDMAEMA-modified SPCE	11nt AQ-labeled acpcPNA (non-immobilized)	SWV	0.35×10^{-9}–35×10^{-9} M	0.13×10^{-9} M	This work

[a] AuE=gold electrode; ITO=indium tin oxide; SPCE=screen print carbon electrode.
[b] Fc=ferrocene; MB=methylene blue; AQ=anthraquinone.

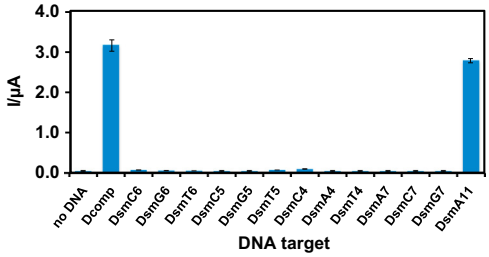

Fig. 3. Specificity test of AQ-PNA (50 nM) with various mismatched DNA (50 nM) in 10 mM Tris–HCl buffer (pH 8.0) under optimized conditions.

efficiently form and be adsorbed by the positively charged electrode. The excellent mismatch discrimination of acpcPNA had been repeatedly demonstrated in prior publications [31–36,38].

3.6. Effects of excess target and non-target DNA

Since both unhybridized and hybridized DNA are negatively charged and can be electrostatically adsorbed by the electrode, any DNA detection platforms that rely on the differential adsorption DNA and PNA–DNA hybrids onto the electrode are subjected to interference by competitive adsorption of free DNA that may result in decreased signal [39]. In the case of complementary DNA target, the signal does decrease when the concentration of the DNA exceeds that of the probe (Section 3.4). In principle, one could solve this problem by increasing the probe concentration in order to avoid the situation of having excess of target DNA over the probe. Next, the effect of non-complementary DNA target was investigated. When non-complementary DNA was added into the solution in 1, 10 and 100 folds relative to the complementary DNA, it competes with the PNA–DNA hybrids in adsorption to the electrode as shown by the decreased electrochemical signals. Nevertheless, a clear signal could still be observed at the amount of non-complementary DNA as high as 100 times to that of the complementary DNA. It should be noted that in all cases, the non-complementary DNA does not contribute to the electrochemical signal even at high concentrations (Fig. 4). The negative effect due to high concentration of unhybridized DNA was also observed in Luo's work [39], which was so pronounced that the signal decreased to $<20\%$ in the presence of 10 equiv. of non-complementary DNA, and almost completely disappeared at 15 equiv. Our sensor is less sensitive to the interference by the non-target DNA, about 50% and 20% of the signal relative to the maximum was retained at 10 and 100 equiv., respectively (Fig. 4). In addition, the possible interferences by proteins were studied using bovine serum albumin (BSA) as a model protein. It was observed that more than 90% of the PNA–DNA signal was retained at BSA concentrations of 0.7% or less. However, at high concentrations of BSA, the signal was suppressed considerably (Fig. S15, SI). Nevertheless, these potential interferences by excess of DNA and proteins should

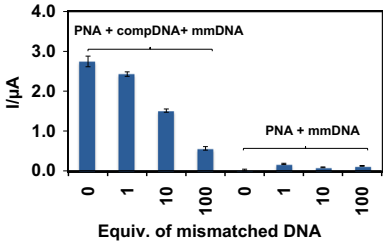

Fig. 4. Effects of non-target DNA to the signal of PNA and complementary PNA–DNA hybrid; concentrations: PNA=50 nM, complementary DNA (Dcomp)=50 or 0 nM and non-target DNA (DsmC)=0, 50, 500 and 5000 nM (0, 1, 10 and 100 equiv.) in 10 mM Tris–HCl buffer (pH 8.0) under optimized conditions.

not negatively affect the analysis of amplified DNA samples, which contain predominantly the DNA target of interest in nanomolar concentration ranges (see Section 3.8).

3.7. Effects of long and duplex target DNA

The situation for detection of real DNA samples will be significantly different from the proof-of-principle experiments above because real DNA samples are usually much longer than the probe and exist as a duplex. The ability of this platform to detect long and duplex DNA targets was therefore investigated. A single stranded 19bp DNA target (ssDcomp19) having a central region that is complementary to the AQ-PNA probe gave comparable signal to the short DNA target, suggesting that the extra hanging part in the DNA strand does not interfere with the detection (Fig. S16A and B, SI). The electrochemical signal was still observed with the duplex DNA target (dsDcomp19) formed by annealing ssDcomp19 and its complementary DNA strand. However, longer times are required for the signal to reach maximum (10 and 20 min in the absence and presence of 100 mM NaCl, respectively). To improve the PNA–DNA binding kinetics, the DNA duplex and PNA was mixed and heated to 90 °C and cooled down, after which the maximum signal was reached immediately. No signals were observed in the analogous experiment carried out with single and double stranded DNA target containing a mismatched base (dsDsmC19), thus confirming the high specificity of the PNA probe (Fig. S16C, SI).

3.8. Detection of real DNA samples

In detection of real DNA samples, the DNA extracted from the shrimp was first amplified by LAMP [44]. This technique was chosen because it offers several advantages over PCR including high specificity, larger amplification factor and the ability to operate at a constant temperature (no need for thermal cycling). The LAMP samples were mixed with the probe before denaturation by heating to 90 °C before cooling down. As shown in Fig. 5A and B, a clear signal was observed with the WSSV-positive sample and not

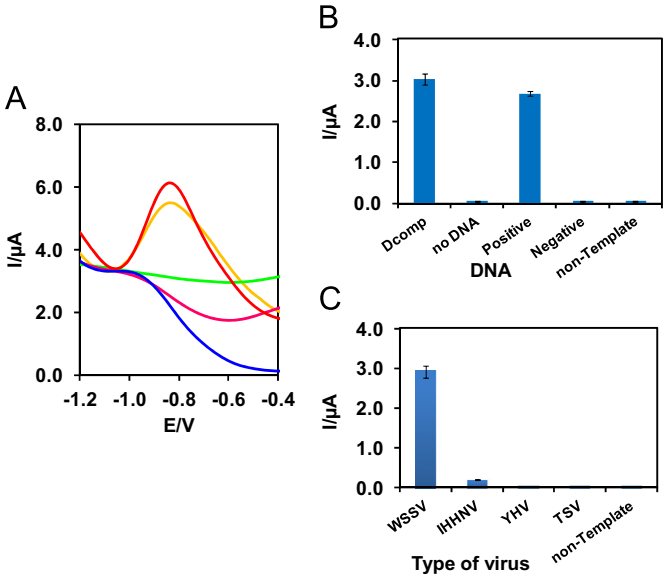

Fig. 5. Comparison of SWV signals [(A) raw data, (B) bar graph] obtained from detection of various LAMP-amplified WSSV samples: positive (orange), negative (pink), non-template control (green), synthetic complementary DNA (Dcomp, red), no DNA (blue) and (C) specificity test for WSSV among other samples including non-template control, IHHNV, YHV and TSV. (For interpretation of the references to color in this figure legend, the reader is referred to the web version of this article.)

Table 3
Comparison of detection limit of this work with other WSSV detection methods.

DNA amplification	Detection	Detection limit	References
PCR	Gel electrophoresis (EtBr staining)	100 pg	[59]
Nested PCR	Gel electrophoresis (EtBr staining)	100 fg	[59]
LAMP	Gel electrophoresis (EtBr staining)	1 fg	[59]
Real-time LAMP	Turbidity	100 copies	[60]
LAMP	Fluorescence (FRET probes)	100 copies	[61]
LAMP	Colorimetric (gold nanoparticles)	200 copies	[62]
Real time, isothermal recombinase polymerase amplification	Fluorescence (SYBR green)	5 copies	[63]
Insulated isothermal PCR	Fluorescence (TaqMan probe)	10 copies	[64]
LAMP	Electrochemical (PNA probe/SPCE)	10 copies	This work

with the negative samples and non-template DNA control.

The specificity of the DNA detection was further studied by comparison of the signals of LAMP samples obtained from various types of shrimp virus including IHHNV, YHV, and TSV. The results suggested that this PNA-based sensor is highly specific and can unambiguously differentiate WSSV from other types of virus (Fig. 5C). Finally, the sensitivity test suggested that in combination with LAMP technique as low as 10 copies of WSSV DNA in the sample could be readily detected (Fig. S17, SI). This level of sensitivity is competitive with other PCR and LAMP-based WSSV DNA assays with optical detection (Table 3). Therefore, the new technique shows a great promise in high throughput analysis of DNA samples.

4. Conclusions

An immobilization-free miniaturized electrochemical platform for DNA sequence detection based on anthraquinone-labeled pyrrolidinyl peptide nucleic acid (AQ-PNA) probe was successfully developed. The working principle involves a differential electrostatic adsorption between PNA and PNA–DNA hybrids onto a screen-printed carbon electrode modified with a positively-charged polymer (PQDMAEMA) that result in a positive signal only when the AQ-PNA is hybridized with the complementary DNA target. Although the same basic principle has been reported and implemented in previous works, the combination of pyrrolidinyl PNA probe and PQDMAEMA-modified screen print carbon electrode for DNA detection in an immobilization-free format is previously unreported. Hence, the ability of the developed DNA sensing platform to exhibit an excellent specificity in discriminating of complementary DNA from various non-complementary, including single-mismatched, DNA targets with a sub-nanomolar detection limit, and its applications in sensitive detection of real DNA samples should be considered as a significant achievement. The immobilization-free procedure means that there is no extra probe immobilization step that is time-consuming (several hours) and requires large excess of probes (usually in the μM range) [15,34]. The amount of probe required for each measurement in this immobilization-free system is very small (1 pmol or less), which compensates for its disposable nature. In addition to the performance, this DNA sensing platform offers significant advantages when compared to other related DNA sensing platforms in terms of operational simplicity, costs and portability. However, one limitation that requires further improvement is the inability to reuse the electrode due to potential loss of the water-soluble linear polymers upon washing, which could be solved by using more highly cross-linked polymers. Another additional limitation is the signal suppression by competitive adsorption of DNA and proteins at high concentrations which could complicate the DNA analysis in the presence of large excess of such interferences. Even with such limitations, the developed sensor was successfully used in combination with LAMP for a rapid and specific detection of WSSV from shrimp DNA with a higher sensitivity than gel- or fluorescence-based detection.

Acknowledgments

The authors would like to acknowledge financial supports from the Thailand Research Fund (DPG5780002) and Center of Innovative Nanotechnology (CIN). We also gratefully acknowledge Dr. Voravee Hoven and Miss Pornpen Sae-ung for kindly providing the PQDMAEMA samples.

Appendix A. Supplementary material

Supplementary data associated with this article can be found in the online version at http://dx.doi.org/10.1016/j.talanta.2015.08.059.

References

[1] D.S. Elenis, D.P. Kalogianni, K. Glynou, P.C. Ioannou, T.K. Christopoulos, Anal. Bioanal. Chem. 392 (2008) 347–354.
[2] I. Palchetti, M. Mascini, Analyst 133 (2008) 846–854.
[3] K. Glynou, P.C. Ioannou, T.K. Christopoulos, V. Syriopoulou, Anal. Chem. 75 (2003) 4155–4160.
[4] V. Gubala, L.F. Harris, A.J. Ricco, M.X. Tan, D.E. Williams, Anal. Chem. 84 (2012) 487–515.
[5] X. Mao, Y. Ma, A. Zhang, L. Zhang, L. Zeng, G. Liu, Anal. Chem. 81 (2009) 1660–1668.
[6] X. Luo, I.M. Hsing, Analyst 134 (2009) 1957–1964.
[7] B.C. Janegitz, J. Cancino, V. Zucolotto, J. Nanosci. Nanotechnol. 14 (2014) 378–389.
[8] M.I. Pividori, A. Merkoçi, S. Alegret, Biosens. Bioelectron. 15 (2000) 290–303.
[9] T.G. Drummond, M.G. Hill, J.K. Barton, Nat. Biotechnol. 10 (2003) 1192–1199.
[10] F. Lucarelli, G. Marrazza, A.P.F. Turner, M. Mascini, Biosens. Bioelectron. 19 (2004) 515–530.
[11] P. de-los-Santos-Álvarez, M.J. Lobo-Castañón, A.J. Miranda-Ordieres, P. Tuñón-Blanco, Anal. Bioanal. Chem. 378 (2004) 104–118.
[12] P. He, Y. Xu, Y. Fang, Anal. Lett. 38 (2005) 2597–2623.
[13] R.Y. Lai, E.T. Lagally, S.-H. Lee, H.T. Soh, K.W. Plaxco, A.J. Heeger, Proc. Natl. Acad. Sci. USA 103 (2006) 4017–4021.
[14] J. Labuda, A.M.O. Brett, G. Evtugyn, M. Fojta, M. Mascini, M. Ozsoz, L. Palchetti, E. Palecek, J. Wang, Pure Appl. Chem. 82 (2010) 1161–1187.
[15] Y. Xiao, X. Qu, K.W. Plaxco, A.J. Heeger, J. Am. Chem. Soc. 129 (2007) 11896–11897.
[16] A. Abi, E.E. Ferapontova, J. Am. Chem. Soc. 134 (2012) 14499–14507.
[17] E. Farjami, L. Clima, K. Gothelf, E.E. Ferapontova, Anal. Chem. 83 (2011) 1594–1602.
[18] H. Cai, X. Cao, Y. Jiang, P. He, Y. Fang, Anal. Bioanal. Chem. 375 (2003) 287–293.
[19] N. Zhu, Z. Chang, P. He, Y. Fang, Anal. Chim. Acta 545 (2005) 21–26.
[20] A. Erdem, P. Papakonstantinou, H. Murphy, M. McMullan, H. Karadeniz, S. Sharma, Electroanalysis 22 (2010) 611–617.
[21] G. Liu, Y. Wan, V. Gau, J. Zhang, L. Wang, S. Song, C. Fan, J. Am. Chem. Soc. 130 (2008) 6820–6825.
[22] H. Fan, Y. Xu, Z. Chang, R. Xing, Q. Wang, P. He, Y. Fang, Biosens. Bioelectron. 26 (2011) 2655–2659.
[23] C. Xu, H. Cai, P.G. He, Y.Z. Fang, Analyst 126 (2001) 62–65.
[24] M. Kobayashi, T. Kusakawa, M. Saito, S. Kaji, M. Oomura, S. Iwabuchi, Y. Morita,

Q. Hasan, E. Tamiya, Electrochem. Commun. 6 (2004) 337–343.
[25] X. Luo, I.M. Hsing, Electrochem. Commun. 13 (2011) 742–745.
[26] F. Xuan, X. Luo, I.M. Hsing, Anal. Chem. 84 (2012) 5216–5220.
[27] F.X.L. Xuan, I.M. Hsing, Biosens. Bioelectron. 35 (2012) 230–234.
[28] C. Briones, M. Moreno, Anal. Bioanal. Chem. 402 (2012) 3071–3089.
[29] C. Vilaivan, C. Srisuwannaket, C. Ananthanawat, C. Suparpprom, J. Kawakami, Y. Yamaguchi, Y. Tanaka, T. Vilaivan, Artif. DNA: PNA XNA 2 (2011) 50–59.
[30] T. Vilaivan, C. Srisuwannaket, Org. Lett. 8 (2006) 1897–1900.
[31] T. Vilaivan, Acc. Chem. Res. 48 (2015) 1645–1656.
[32] C. Ananthanawat, T. Vilaivan, V.P. Hoven, X. Su, Biosens. Bioelectron. 25 (2010) 1064–1069.
[33] W. Janrungroatsakul, T. Vilaivan, C. Vilaivan, S. Watchasit, C. Suksai, W. Ngeontae, W. Aeungmaitrepirom, T. Tuntulani, Talanta 105 (2013) 1–7.
[34] S. Sankoh, S. Samanman, O. Thipmanee, A. Numnuam, W. Limbut, P. Kanatharana, T. Vilaivan, P. Thavarungkul, Sens. Actuators B 177 (2013) 543–554.
[35] O. Thipmanee, S. Samanman, S. Sankoh, A. Numnuam, W. Limbut, P. Kanatharana, T. Vilaivan, P. Thavarungkul, Biosens. Bioelectron. 38 (2012) 430–435.
[36] S. Jampasa, W. Wonsawat, N. Rodthongkum, W. Siangproh, P. Yanatatsaneejit, T. Vilaivan, O. Chailapakul, Biosens. Bioelectron. 54 (2014) 428–434.
[37] K. Kerman, M. Vestergaard, N. Nagatani, Y. Takamura, E. Tamiya, Anal. Chem. 78 (2006) 2182–2189.
[38] B. Boontha, J. Nakkuntod, N. Hirankarn, P. Chaumpluk, T. Vilaivan, Anal. Chem. 80 (2008) 8178–8186.
[39] X. Luo, T.H. Lee, I.M. Hsing, Anal. Chem. 80 (2008) 7341–7346.
[40] X. Luo, I.M. Hsing, Electroanalysis 21 (2009) 1557–1561.
[41] X. Luo, I.M. Hsing, Biosens. Bioelectron. 25 (2009) 803–808.
[42] C.M. Escobedo-Bonilla, V. Alday-Sanz, M. Wille, P. Sorgeloos, M.B. Pensaert, H. J. Nauwynck, J. Fish Dis. 31 (2008) 1–18.
[43] E. Khaled, H.N.A. Hassan, A. Girgis, R. Metelka, Talanta 77 (2008) 737–743.
[44] T. Notomi, H. Okayama, H. Masubuchi, T. Yonekawa, K. Watanabe, N. Amino, T. Hase, Nucleic Acids Res. 28 (2000) e63.
[45] ⟨http://www6.appliedbiosystems.com/support/tutorials/pdf/quant_pcr.pdf⟩, accessed 27.07.14.
[46] L.M. Nunan, D.V. Lightner, J. Virol. Methods 171 (2011) 318–321.
[47] J. Sambrook, E.F. Fritsch, T. Maniatis, Molecular Cloning: A Laboratory Manual, 2nd ed., Cold Spring Harbor Laboratory Press, Plainview, New York, 1989.
[48] S. Kumamoto, M. Watanabe, N. Kawakami, M. Nakamura, K. Yamana, Bioconjugate Chem. 19 (2008) 65–69.
[49] M.T. Tierney, M.W. Grinstaff, J. Org. Chem. 65 (2000) 5355–5359.
[50] J. Wang, M. Pedrero, H. Sakslund, O. Hammerich, J. Pingarron, Analyst 121 (1996) 345–350.
[51] E. Khaled, H.N.A. Hassan, I.H.I. Habib, R. Metelka, Int. J. Electrochem. Sci. 5 (2010) 158–167.
[52] W. Cao, C.J. Easley, J.P. Ferrance, J.P. Landers, Anal. Chem. 78 (2006) 7222–7228.
[53] M. Lazerges, F. Bedioui, Anal. Bioanal. Chem. 405 (2013) 3705–3714.
[54] S. Liu, Y. Lin, L. Wang, T. Liu, C. Cheng, W. Wei, B. Tang, Anal. Chem. 86 (2014) 4008–4015.
[55] J. Zhuang, D. Tang, W. Lai, G. Chen, H. Yang, Anal. Chem. 86 (2014) 8400–8407.
[56] A.I.K. Lao, X. Su, K.M.M. Aung, Biosens. Bioelectron. 24 (2009) 1717–1722.
[57] M. Inouye, R. Ikeda, M. Takase, T. Tsuri, J. Chiba, Proc. Natl. Acad. Sci. USA 102 (2005) 11606–11610.
[58] G.L. Igloi, Proc Natl. Acad. Sci. USA 95 (1998) 8562–8567.
[59] T. Kono, R. Savan, M. Sakai, T. Itami, J. Virol. Methods 115 (2004) 59–65.
[60] T. Mekata, R. Sudhakaran, T. Kono, K. Supamattaya, N.T. Linh, M. Sakai, T. Itami, Lett. Appl. Microbiol. 48 (2009) 25–32.
[61] P.H. Chou, Y.C. Lin, P.H. Teng, C.L. Chen, P.Y. Lee, J. Virol. Methods 173 (2011) 67–74.
[62] Y. Seetang-Nun, W. Jaroenram, S. Sriurairatana, R. Suebsing, W. Kiatpathomchai, Mol. Cell. Probes 27 (2013) 71–79.
[63] X. Xia, Y. Yu, M. Weidmann, Y. Pan, S. Yan, Y. Wang, PLoS One 9 (2014) e104667.
[64] Y.-L. Tsai, H.-T.T. Wang, H.-F.G. Chang, C.-F. Tsai, C.-K. Lin, P.-H. Teng, C. Su, C.-C. Jeng, P.-Y. Lee, PLoS One 7 (2014) e45278.